

Patterns of Evolutionary Divergence and Convergence in the Bushy-Tailed Woodrat (*Neotoma cinerea*) Across Western North America

Angela D. Hornsby · Marjorie D. Matocq

© Springer Science+Business Media New York 2013

Abstract The degree of concordance between patterns of divergence in genetic and morphological characters provides insight into the process of evolutionary diversification. We analyzed species-wide morphological variation in a broadly distributed species of small mammal, the bushy-tailed woodrat (*Neotoma cinerea*), for comparison against a recently developed mitochondrial phylogeny. We focused our analyses on patterns of qualitative and quantitative craniodental morphological variation throughout the distribution of this taxon. We found strong concordance between the morphology of one prominent craniodental feature (sphenopalatine vacuity) and the major mitochondrial lineages, but only minimal differentiation in overall morphometric variation between these clades. Further, in contrast to the largely east–west subdivision of mitochondrial and sphenopalatine vacuity variation, cluster analyses of morphometric variation revealed a north–south morphological subdivision irrespective of mitochondrial clade. Our combined character sets are best explained by a deep history of evolutionary divergence within this taxon accompanied or followed by broad-scale convergent or parallel evolution.

Keywords Convergent evolution · Morphology · Morphometry · *Neotoma* · Parallel evolution · Rodent

Electronic supplementary material The online version of this article (doi:10.1007/s10914-013-9232-7) contains supplementary material, which is available to authorized users.

A. D. Hornsby (✉) · M. D. Matocq
Program in Ecology, Evolution, and Conservation Biology,
Department of Natural Resources and Environmental Science,
University of Nevada, 1664 N. Virginia St.,
Reno, NV 89557, USA
e-mail: adhornsby@gmail.com

Introduction

Patterns of morphological variation are important to understanding how groups are related to one another, how they function in ecosystems, and how they evolve to meet environmental challenges. While molecular methods continue to provide unprecedented insight into biogeographic and demographic history (Drummond et al. 2005; Lemey et al. 2009; Hey 2010), only by combining genetic and morphological perspectives can we begin to understand how intrinsic (e.g., genomic) and extrinsic (e.g., environmental) factors interact to determine the evolution of phenotypic variation. When comparing genetic and morphological patterns between species or higher taxonomic levels, the basic expectation is that lineages that are no longer exchanging alleles will show genetic and phenotypic divergence over evolutionary time through a combination of mutation, drift, and, perhaps selection. That is, without gene flow, the null expectation is of divergence between taxonomic units and concordance among multiple character sets between those units. Nonetheless, much is to be learned about the evolutionary process when character sets are unexpectedly discordant. An example of this is cryptic speciation, in which lineages are morphologically indistinguishable but show deep genetic divergence or are otherwise reproductively isolated (e.g., Baker 1984; Derkarabetian et al. 2011; Smith et al. 2011). These patterns may be due to combinations of factors such as genomic events causing instantaneous speciation (Rieseberg and Willis 2007), differences in non-morphological factors such as mating calls, or stabilizing selection on morphology following divergence (Bickford et al. 2007). At the other extreme, taxa may be hyper-diverse morphologically but comprise a shared gene pool or show limited overall genetic variation. These patterns may be due to localized selective sweeps causing divergence at loci

affecting morphology but not overall in the genome (e.g., Hillis et al. 1991) or due to the influence of phenotypic plasticity or epigenetic controls on phenotype (e.g., Adams et al. 2003). Convergent evolution can also produce discordant patterns as species radiations fill open niche spaces, famously illustrated in the *Anolis* lizard species complex, which shows independent evolution of similar ecomorphs among geographically isolated clades (Losos et al. 1998), and in East African cichlid fishes, which show convergent morphologies between lineages in different lakes (Kocher et al. 1993).

We recently developed a mitochondrial phylogeny (Hornsby and Matocq 2012) for the wide-ranging bushy-tailed woodrat, *Neotoma cinerea*. The aims of this study are to quantify morphological patterns of variation in this taxon and compare these to major patterns of genetic variation.

From the mtDNA phylogeny we identified two reciprocally monophyletic and nearly allopatric clades separated by the Green and Colorado rivers, with the Eastern clade occupying the Rocky Mountains east of the Colorado and Green rivers, and the Western clade occupying regions west of the Green and Colorado rivers as well as the northern Rocky Mountains (Fig. 1a). We estimated that these clades diverged 2.77 million years ago (95 % highest probability density 2.17 to 3.41 million years ago), with an average uncorrected cytochrome *b* (*cyt b*) sequence p-distance of 6.5 % and corrected (GTR+I+ Γ) divergence of 8.8 %. Although the geographic diversity of *N. cinerea* has been appreciated for a long time (e.g., Coues 1877; Goldman 1910; Hooper 1940), we are now in a position to begin putting morphological patterns in the context of genetic patterns to determine whether patterns of divergence in one are echoed in the other.

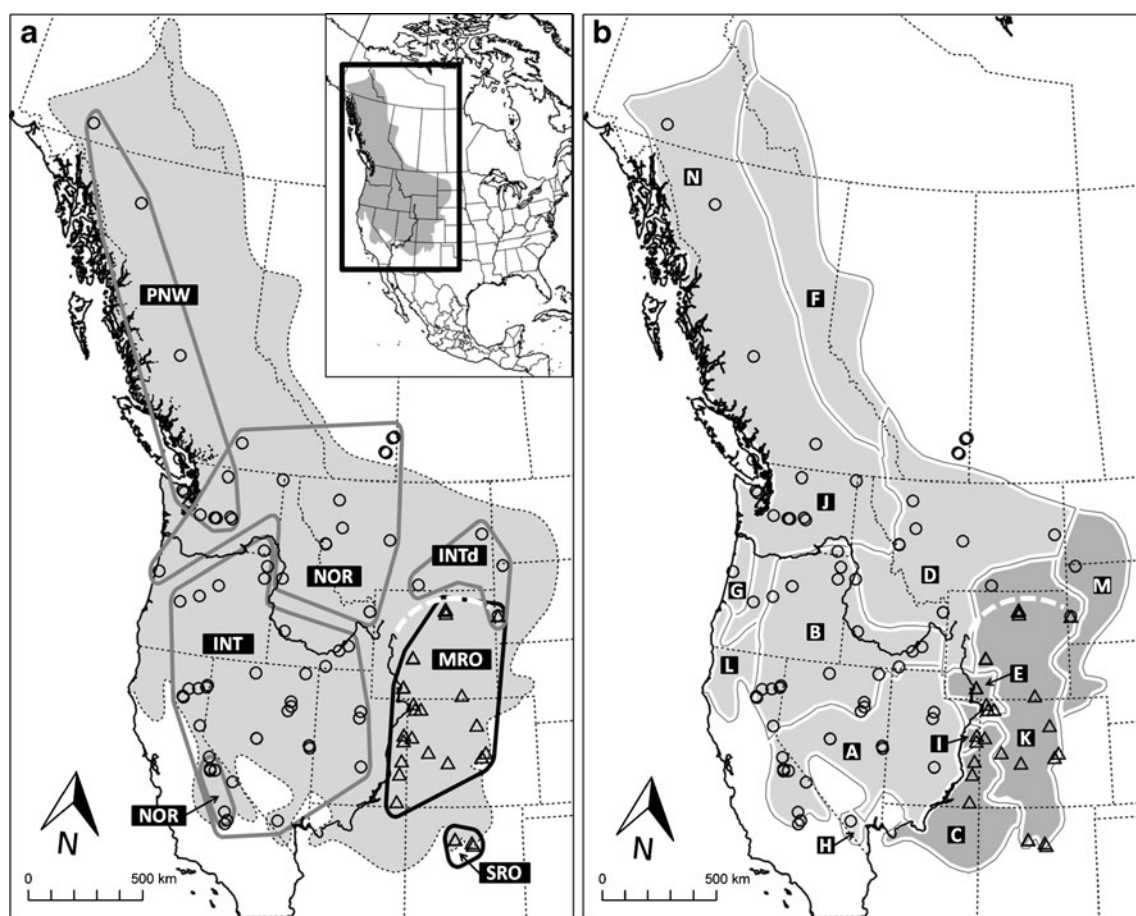


Fig. 1 Clades and subspecies of *Neotoma cinerea* in western North America. **a** major *cyt b* clades and subclades adapted from Hornsby and Matocq (2012). Heavy black lines delineate Eastern clade subclades (SRO and MRO), and heavy grey lines delineate Western clade subclades (PNW, NOR, and INT including disjunct INTd). The range of *N. cinerea* is shaded grey. **b** subspecies based on Goldman (1910) and separated from *N. c. occidentalis* by the white dashed line. Subspecies are labeled by letters: A, *acraea*; B, *alticola*; C, *arizonae*; D, *cinerea*; E, *cinnamomea*; F, *drummondii*; G, *fusca*; H, *lucida*; I, *macrodon*; J, *occidentalis*; K,

oroletes; L, *pulla*; M, *rupicola*; and N, *saxamans*. Subspecies are colored according to historically hypothesized major groups: *N. c. oroletes* group, dark grey; *N. c. occidentalis* group, light grey. In both panels, specimens of the two major phylogenetic clades are represented with triangles (Eastern clade) and circles (Western clade), the white dashed line is the approximate boundary between the two major phylogenetic clades, and solid black lines show the Columbia and Snake rivers in the northwest and the Green and Colorado rivers in the southeast

We briefly summarize historical studies of *N. cinerea* morphology, both to introduce previously identified patterns and to place our work within this context. *Neotoma cinerea* is classified under the monotypic subgenus *Teonoma* (Gray 1843; Goldman 1910; Edwards and Bradley 2002) and has 17 named taxa which are currently recognized under 13 subspecies (Hall 1981; Carleton and Musser 2005; Fig. 1b). Coues (1877) and later Merriam (1893) noted potential differences between *N. cinerea* in the east versus west of the species range. The most cogent difference was a pair of large gaps on the ventral skull, posterior to the hard palate between the sphenoid and palatine bones, which Merriam termed sphenopalatine vacuities (SPVs; Merriam 1893; Fig. 2). SPVs are open in all *Neotoma* (although sometimes variable in size; Allen 1894a; Merriam 1894a; True 1894), except for in western *N. cinerea* where they are usually fused closed by medial extensions of the palatines (Merriam 1894a). This difference in SPV morphology became the basis for distinguishing two major groups of *N. cinerea*, which were loosely (and contrary to conventions on nomenclatural precedence) referred to by some authors as the *N. c. orolestes* group (e.g., Allen 1894b, 1895), which consisted of subspecies with open SPVs and that occupied the southern Rocky Mountain region, and *N. c. occidentalis* group (e.g., True 1894), which consisted of subspecies with usually narrow or closed SPVs and that occupied the northern Rocky Mountains and Intermountain West. Although this systematic difference was recognized in one of the major *Neotoma* taxonomic revisions (Goldman 1910), contemporary species-wide descriptions of *N. cinerea* note SPVs simply as either present or absent without specific regard to geography (Hall 1981; Smith 1997).

While SPV morphology was used to differentiate these two larger *N. cinerea* groups, more attention was focused on body size, pelage, and particularly craniodental patterns to summarize overall geographic variation. Some features such as body size (Goldman 1910, 1917; Hooper 1940) and auditory bullae size (Merriam 1893; Goldman 1910; Hooper 1940, 1944) appear to vary gradually across the species range. Other features such as pelage color (Hooper 1940), molar row length (Baird 1857; Hooper 1940; Kelson 1949), zygomatic breadth (Goldman 1917; Hooper 1940), and interorbital constriction (Osgood 1900; Goldman 1910) were also noted in some taxonomic descriptions, but not as consistently, so range-wide patterns have not been identified. These morphological features were often used to delimit subspecies, though the observation that almost all adjacent *N. cinerea* subspecies appear to broadly intergrade (Coues 1877; Allen 1903; Goldman 1910; Burt 1934; Hooper 1940; Finley 1958) meant that there were few steep clines with which to define subspecies boundaries. The exceptions to this are between taxa separated by major geographic barriers, such as *N. c. arizonae* and *N. c. macrodon* separated from *N. c. acraea* by the Colorado River (sensu Goldman 1910; Kelson 1949), and

N. c. fusca partly separated from *N. c. occidentalis* by the Columbia River (Hooper 1940).

Here, we use both qualitative and quantitative morphological analyses to inform our understanding of the evolutionary history of *N. cinerea* and the relationship between major patterns of genetic and morphological variation. Specifically, we ask: (1) what are the geographic patterns of qualitative and quantitative craniodental variation throughout the species range, (2) are patterns of morphological variation concordant with the two major mitochondrial clades, and (3) how is morphometric variation among smaller geographic units (i.e., subspecies) related to patterns between the two major clades? We utilize subspecies in some analyses to represent convenient partitions of geographic variation and to relate our work back to historical descriptions, but our intent is neither to capture the full extent of variation within these units nor to assess their taxonomic validity.

Materials and Methods

Specimens Examined

We examined specimens of age classes 2 to 4 ($n=405$, Online Resource 1) as determined by degree of wear on the upper molars (Matocq 2002). The youngest specimens representing age class 1 were excluded because they are most likely to differ from other classes due to ontogenetic changes in morphology (e.g., developmental allometry), including changes in SPV relative to adult forms (Allen 1894a).

We measured all specimens with associated cyt *b* sequences, as well as specimens occurring in “skull populations.” For phylogeny-based analyses, specimens were classified as belonging to the Eastern or Western cyt *b* clades based on a Bayesian phylogeny of complete cyt *b* sequences (Hornsby and Matocq 2012). Specimens without associated cyt *b* sequences were assigned to one of the two major clades based on geographic position. We also classified specimens by subspecies and skull population. Subspecies identifications were based on geographic limits in Hall (1981), though we chose to include *N. c. saxamans* (currently synonymized with *N. c. occidentalis*; Cowan and Guiguet 1956) and based its distribution on Goldman (1910). Skull populations ($n=25$) were defined as groups of specimens collected within 15 km (7.5 km radius) of one another, and lacking major discernible barriers such as rivers between collection sites. Because juvenile *N. cinerea* are known to disperse up to 3 km from their natal site (Escherich 1981), we consider 15 km sufficient to meet our assumption that groups

represent panmictic populations. The subspecies categorized within the *N. c. orolestes* and *N. c. occidentalis* groups, and number of skull populations representing each, are as follows: *N. c. orolestes* group (total skull populations, $n=8$): *N. c. arizonae* ($n=2$), *N. c. cinnamomea* ($n=2$), and *N. c. orolestes* ($n=4$); *N. c. occidentalis* group (total skull populations, $n=17$): *N. c. acraea* ($n=6$), *N. c. alticola* ($n=3$), *N. c. cinerea* ($n=1$), *N. c. fusca* ($n=1$), *N. c. occidentalis* ($n=3$), *N. c. pulla* ($n=1$), and *N. c. saxamans* ($n=2$). The subspecies for which sample sizes were inadequate include: *N. c. orolestes* group *N. c. macrodon* and *N. c. rupicola*; and *N. c. occidentalis* group *N. c. drummondii* and *N. c. lucida*.

Measurements and Size Corrections

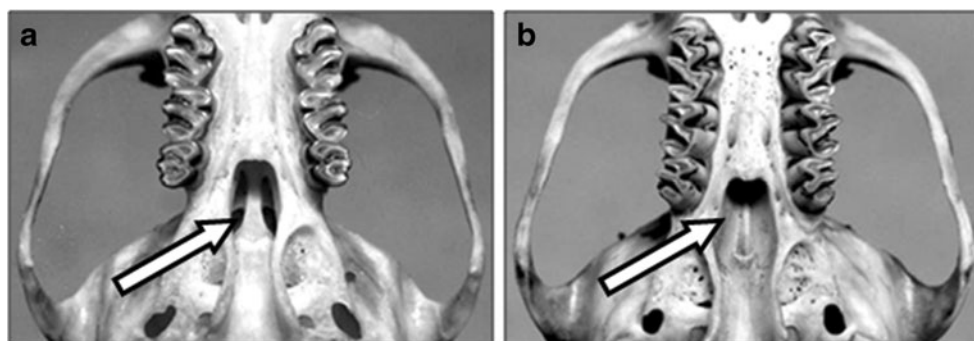
We classified SPVs of all specimens into one of three qualitative states as suggested by Hooper (1940): open (> 0.2 mm; Fig. 2a); narrow (≤ 0.2 mm); or closed (absent; Fig. 2b). For morphometric analyses, we measured 11 linear variables from *N. cinerea* skulls using digital calipers with precision to 0.01 mm: length of nasals; rostrum width; rostrum depth; interorbital breadth; length of palatal bridge; alveolar length of molar row; zygomatic breadth; occipital breadth at mastoid processes; auditory bullar length; width of interpterygoid fossa; and basilar length (Matocq and Murphy 2007). Basilar length was used to represent overall body size and serve as a scaling factor for the other ten variables. To confirm that basilar skull length is a reasonable proxy for body size, we performed regression analyses of basilar length against total length (mm), head and body length (mm), and weight (g) taken from specimen records. All morphometric analyses were performed in R v2.13.0 (R Core Development Team 2011).

Because *N. cinerea* shows sexual size dimorphism (Smith 1997), initial analyses of quantitative variables were performed separately for each sex. To determine whether there were differences among age classes that could preclude pooling specimens for further analyses, we performed ANOVAs for each measurement in each

sex with age as the predictor variable. To specify which age classes, if any, differed, we performed Tukey-Kramer multiple comparisons between each pair of age classes. Based on the results, we omitted specimens of age class 2 and pooled age classes 3 and 4 in each sex for morphometric analyses (see Results).

To account for potential allometry in relation to overall specimen size, we applied a regression-based size adjustment (Thorpe 1975). Though more mathematically intensive than methods that account for body size by calculating proportions or allowing size to dominate the first vector of multivariate analyses, regression methods are considered to better account for ontogenetic variation correlated with body size (Thorpe 1976; Reist 1985). This method adjusts values with respect to the slope (β) derived from a regression of each variable against body size (i.e., basilar length) by rotating the regression slope so that $\beta=0$. Adjusted values of perfectly isometric variables (coefficient of allometry=1) are equivalent to proportions, adjusted values of variables showing varying degrees of allometry (coefficient of allometry $\neq 1$) are corrected based on their relationship with size, and variables showing no relationship with size (coefficient of allometry=0) are not adjusted. The result is adjusted values that are either unusually small or unusually large given the specimen size, based on the residuals of the regression model. This method can be problematic if there is geographic variation in both body size and in the allometric relationship between each variable and size; in this case, using respective within-population regressions for correction are more appropriate than applying a single pooled regression which assumes the same allometric relationship across all populations (Thorpe 1976). To determine whether separate or pooled regressions were warranted, we constructed general linear models for each variable in each sex with predictors (1) basilar length, and (2) geographic proxy, for which we ran general linear models using latitude and longitude (continuous variables) or skull population (categorical variable), respectively. We interpreted a lack of significant interaction effects as support that the allometric relationship

Fig. 2 Extremes of *N. cinerea* sphenopalatine vacuity (SPV) morphology as seen on the ventral skull. Both specimens are from the Brigham Young University Monte L. Bean Life Science Museum (BYU). **a** open SPVs, BYU 16618, female, Uintah Co., Utah, *N. c. orolestes* group. **b** closed SPVs, BYU 13888, female, Wasatch Co., Utah, *N. c. occidentalis* group



between each variable and basilar length was consistent across geographic space. Based on the results of these models, we calculated and applied pooled regression slopes for size adjustments (see [Results](#)).

We regressed each variable for each sex against basilar length, and adjusted variables with slopes of at least marginal significance ($P \leq 0.1$). Adjusted values were calculated by applying the regression β in the formula $Y_{i,adj} = Y_i - \beta(X_i - \bar{X})$, where $Y_{i,adj}$ is the adjusted measurement value, Y_i is the original measurement value, X_i is the basilar length, and \bar{X} is the mean basilar length within the sex (Thorpe 1975). Measurements were not size-adjusted if the regression model was not at least marginally significant. We standardized adjusted values into Z-scores with the formula $Z = (Y_{i,adj} - \bar{Y}_{i,adj})/s$ where $\bar{Y}_{i,adj}$ is the mean adjusted measurement within the sex and s is the standard deviation of the adjusted measurement within the sex. To determine whether Z-scores of males and females could be pooled, we performed an ANCOVA for each set of original measurements using sex and basilar length as the predictor variables. We interpreted a lack of significant interaction effects as an indication that the linear relationships between each variable and basilar length were consistent between sexes. Based on the ANCOVA model results, we pooled Z-scores of both sexes for further analyses (see [Results](#)). For analyses including uncorrected basilar length, we standardized basilar length in each sex and then pooled the sexes.

Morphological Analyses

To determine the geographic patterns of craniodental variation (question 1), we mapped the SPV state of each specimen geographically ($n=378$) and performed non-hierarchical k -means cluster analyses using the morphometric data. For this analysis, we grouped specimens in $n=25$ skull populations, excluding specimens that did not fall within a population range. We averaged the ten Z-score variables (basilar length excluded) within each population and performed cluster analyses with user-defined group numbers (k) of $k=2$ through $k=5$. As k -means clustering is not hierarchical, each analysis represents the partitioning which maximizes similarity within the k groups without regard to optimal clusterings at other levels of k .

To determine whether the craniodental patterns are concordant with the two major phylogenetic clades (question 2), we mapped the SPV state of each specimen phylogenetically ($n=104$) using a Bayesian phylogeny from complete *cyt b* sequences (1,143 bp) and methods as per Hornsby and Matocq (2012). We also assessed morphometric differences between the two clades using uni- and multivariate statistics. We tested for differences in each variable and in basilar length using Welch's t -tests for unequal variances with Bonferroni corrections for 11 comparisons. Because *N.*

cinerea exhibits latitudinal size variation that conforms to Bergmann's Rule (Bergmann 1847; Brown and Lee 1969; Smith et al. 1995; Smith and Betancourt 2006) and the mitochondrial clades have different latitudinal extents, we also used an ANCOVA model to assess basilar length as a function of both clade and latitude. To investigate multivariate separation and summarize overall variation in the ten Z-score variables (basilar length excluded), we performed a principal component analysis (PCA). From this analysis, we determined the inflection point in the proportion of variation explained across principal components (see [Results](#)) and included all components above this point in a MANOVA model. This assessed the component score for each specimen as a function of clade, helping to quantify the separation of the clades in PCA multivariate space. We also summarized overall variation using a priori clade assignments in a linear discriminant function analysis (DFA) of the ten Z-score variables with jackknife cross-validation to assess classification accuracy.

Lastly, to determine how morphological variation among subspecies is related to patterns between the two major clades (question 3), we performed post-hoc Tukey-Kramer pairwise contrasts of each variable and basilar length in all subspecies with $n \geq 3$ (thus omitting *N. c. drummondii*, *N. c. lucida*, and *N. c. rupicola*). We also compared the proportion of each SPV form within subspecies to historical descriptions (Table 1).

Results

Measurements and Size Corrections

Basilar length is a proxy for body size measurements in *N. cinerea*, including total length ($P < 0.001$, $df=71$, $R^2=0.74$), head and body length ($P < 0.001$, $df=71$, $R^2=0.67$), and weight ($P < 0.001$, $df=60$, $R^2=0.77$), making it reasonable for size corrections of the other morphometric variables.

Significant Tukey-Kramer pairwise differences were evident between age classes 2 vs. 3 and 2 vs. 4 (but not 3 vs. 4) in both sexes for most measurements. Exceptions included (1) interorbital breadth, which was not significant between any age classes in either sex, (2) width of interpterygoid fossa, which was not significant between any age classes within females, and (3) molar row, which was significantly different between age classes 3 vs. 4 in both sexes. We chose to pool data from age classes 3 to 4 within each sex and discard specimens of age class 2 from analyses, satisfying the overall data trends as well as exceptions (1) and (2) above. Because we saw no evident geographic, phylogenetic, or sex biases in age sampling, we pooled molar row data in age classes 3 to 4 as in all other measurements. This yielded a total $n=243$ specimens (149 females, 94 males) of

Table 1 Proportion of *N. cinerea* specimens displaying each category of sphenopalatine vacuity (SPV) morphology: 0 = closed; 1 = narrow; 2 = open. The major clades are further divided into their constituentsubspecies, including *N. c. saxamans* that is currently synonymized with *N. c. occidentalis*. Shaded cells indicate the expected SPV states as suggested by referenced historical literature

Clade	Subspecies	n	Proportion (%)			References
			SPV = 0	SPV = 1	SPV = 2	
Eastern (<i>N. c. orolestes</i> group)	TOTAL	102	0	3	97	
	<i>N. c. arizonae</i>	10	0	0	100	(Merriam 1893; Goldman 1910)
	<i>N. c. cinnamomea</i>	22	0	0	100	(Goldman 1910; Hooper 1944)
	<i>N. c. macrodon</i>	4	0	0	100	(Kelson 1949)
	<i>N. c. orolestes</i>	61	0	3	97	(Merriam 1894b; Goldman 1910)
	<i>N. c. rupicola</i>	5	0	20	80	(Allen 1894b; Goldman 1910)
Western (<i>N. c. occidentalis</i> group)	TOTAL	276	75	21	4	
	<i>N. c. acraea</i>	88	97	3	0	(Goldman 1910; Hooper 1940)
	<i>N. c. alticola</i>	78	88	12	0	(Hooper 1940)
	<i>N. c. cinerea</i>	18	28	67	6	(Goldman 1910; Hooper 1940)
	<i>N. c. drummondii</i>	15	40	60	0	(Goldman 1910; Cowan and Guiguet 1956)
	<i>N. c. fusca</i>	9	89	11	0	(Goldman 1910; Hooper 1940)
	<i>N. c. lucida</i>	2	100	0	0	(Goldman 1917; Hooper 1940)
	<i>N. c. occidentalis</i>	36	67	31	3	(Goldman 1910; Hooper 1940)
	<i>N. c. pulla</i>	12	33	67	0	(Hooper 1940)
<i>N. c. saxamans</i>	18	22	28	50	(Osgood 1900; Goldman 1910)	

age classes 3 to 4 for analyses of quantitative variables. Our general linear models comparing allometric relationships across geographic space as measured by latitude and longitude showed insignificant ($P > 0.1$) interactions between each variable and overall size in both sexes, with the exception of female interorbital breadth ($0.033 < P < 0.048$). Our models using population as a geographic term similarly showed insignificant interactions with the exception of male bullar length ($P = 0.030$). As these were the only measurements with interaction effects and we employed no correction for the inflated chance of Type II error across this set of comparisons, we chose to calculate and apply pooled regression slopes for all measurements and sexes for consistency. All measurements showed at least marginally significant relationships with basilar length and were size-adjusted, with the exception of interorbital breadth which was not significantly related to overall size in either sex (females: $P = 0.146$, $df = 144$; males $P = 0.236$, $df = 90$). We found no significant interactions between sex and basilar length as determinants of measurement size, and therefore pooled sexes after size correction and standardization.

Morphological Analyses

Our first question was aimed at determining the geographic patterns of craniodental variation. SPVs show a shift from open to closed forms in association with the Green and Colorado rivers (Fig. 3a), with closed SPVs to the immediate west of these rivers and open SPVs to the east. Open SPVs were also predominant in the far north of the species

range, while the intermediate narrow form was common through Montana, northern California, and parts of the Pacific Northwest. In k -means cluster analysis of the morphometric data, the skull populations were separated largely into northern and southern groups at $k = 2$ (Fig. 4a). At $k = 3$, the southern group was split into two discontinuous subgroups (Fig. 4b). At $k = 4$, three of the northernmost populations were split from the northern group (Fig. 4c). At $k = 5$, the southern group was split into additional discontinuous subgroups (Fig. 4d). Across levels of k , the persistent units appear to be (1) a southern cluster (with discontinuous internal subdivisions) consisting of southern and eastern *N. cinerea* populations, (2) a far northern cluster consisting of three of the northernmost populations, and (3) a western cluster consisting of the remaining populations west of the Colorado and Green rivers.

Our second question was whether patterns of morphological variation were concordant with the two major phylogenetic clades. As previously described (Hornsby and Matocq 2012), the *cyt b* phylogeny of *N. cinerea* shows two mitochondrial clades occupying the southern Rocky Mountains (Eastern clade) and northern Rocky Mountains and Intermountain West (Western clade), respectively, with one known point of sympatry in western South Dakota (Fig. 1). These clades are further divided into subclades (Hornsby and Matocq 2012), and the subspecies primarily associated with each clade are as follows: Eastern clade: SRO, *N. c. orolestes*; MRO, *N. c. arizonae*, *N. c. cinnamomea*, *N. c. macrodon*, and *N. c. orolestes*; Western clade: PNW, *N. c. occidentalis* and *N. c. saxamans*; NOR, *N. c. cinerea*, *N. c.*

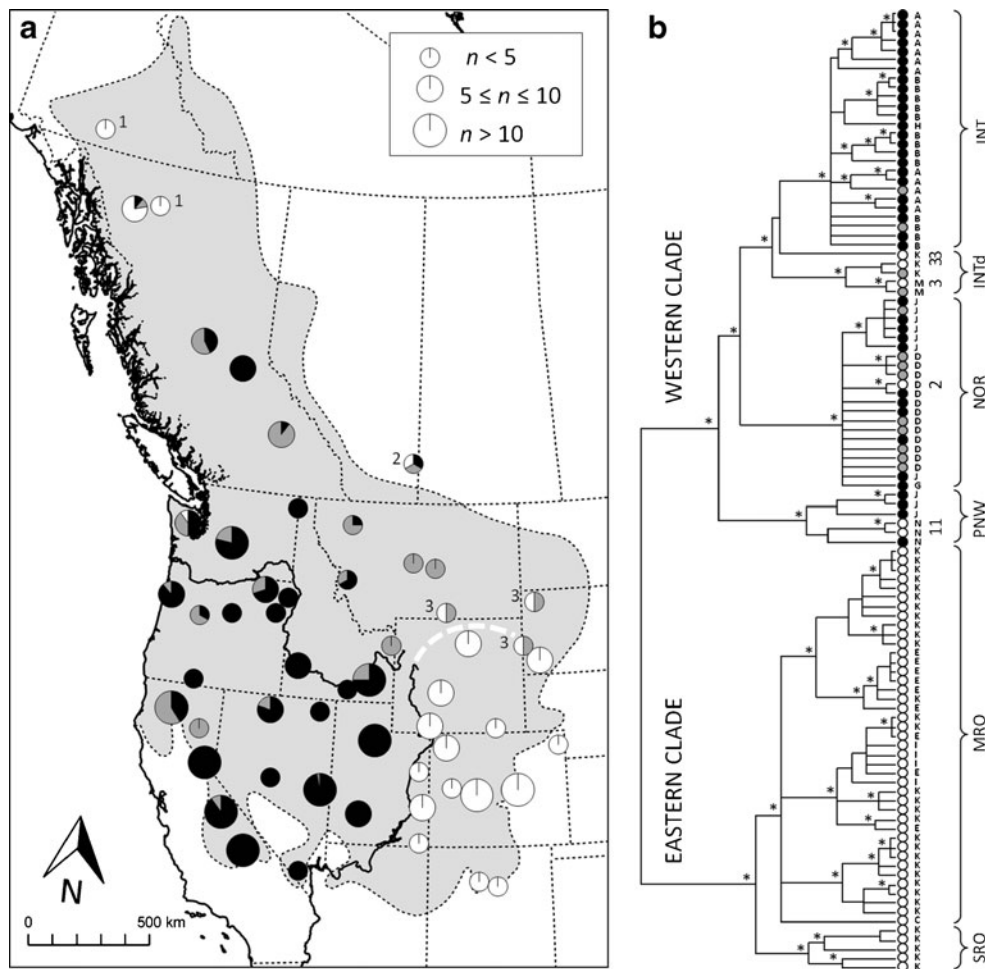


Fig. 3 Geographic and phylogenetic distributions of sphenopalatine vacuity (SPV) morphology in *N. cinerea* in western North America. Pie charts and tip symbols are colored according to SPV morphology: white, open; grey, narrow; black, closed. **a** map of SPV morphology across the *N. cinerea* range (shaded grey), with pie charts showing the proportion of skulls exhibiting each SPV morphology. Pie size corresponds to sample size according to the legend. The white dashed line is the approximate boundary between the two major phylogenetic clades. The solid black lines show the Columbia and Snake rivers in

the northwest and the Green and Colorado rivers in the southeast. **b** ultrametric majority-rule Bayesian phylogeny of individual *cyt b* sequences, including the major Eastern and Western clades and their constituent subclades (Hornsby and Matocq 2012). Nodes with posterior probabilities ≥ 90 are labeled with asterisks. Tips are labeled by subspecies, as coded in Fig. 1. In both panels, groups of specimens in the Western clade but exhibiting open SPVs are coded with numbers to show their phylogenetic and geographic positions

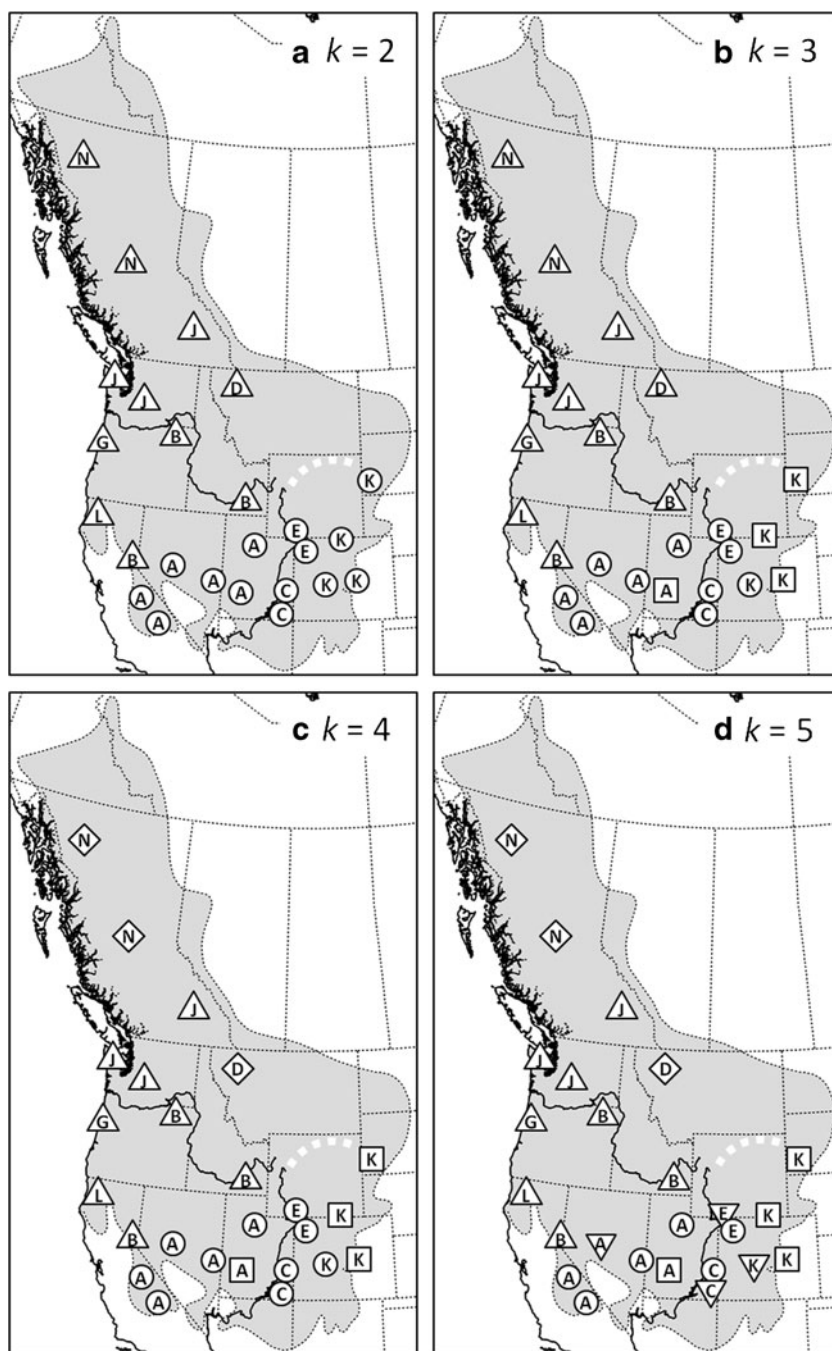
fusca, and *N. c. occidentalis*; INT, *N. c. acraea*, *N. c. alticola*, and *N. c. lucida*. Additionally, the geographic disjunct of INT (INTd) involves individuals of *N. c. cinerea*, *N. c. orolestes*, and *N. c. rupicola* (Fig. 1).

The phylogeny shows different SPV states associated with the major clades, with all Eastern clade specimens showing open SPVs and most Western clade specimens showing closed or narrow SPVs (Fig. 3b). By extension, the major phylogenetic clades are consistent with the *N. c. orolestes* (Eastern clade) and *N. c. occidentalis* (Western clade) groups, which were defined by these SPV states. The exceptions to these general associations of SPV and phylogeography include: (1) PNW subclade *N. c. saxamans* specimens with open SPVs (coded as 1 in Fig. 3); (2) one NOR subclade specimen with open SPVs (coded as 2 in

Fig. 3); and (3) three INTd subclade samples with open SPVs and which fall along the approximate interface of the two major clades (coded as 3 in Fig. 3).

In regard to whether the two clades differ morphometrically, *t*-test comparisons showed significant differences between the Eastern and Western clade specimens for three variables: the Eastern clade has longer auditory bullae ($t_{df=73.8}=6.10$, $P<0.001$), the Western clade has wider interpterygoid fossae ($t_{df=72.7}=-3.29$, $P=0.002$), and the Western clade is larger overall (basilar length, $t_{df=66.6}=-3.81$, $P<0.001$) (Table 2). Although the Western clade specimens have longer basilar lengths, the ANCOVA model showed that latitude has a greater influence ($t_{df=230}=1.82$, $P=0.070$) than clade ($t_{df=230}=0.78$, $P=0.436$). Because *N. cinerea* conforms to Bergmann's Rule in attaining larger

Fig. 4 Geographic distribution of *N. cinerea* groups from *k*-means population clustering at *k*=2 through *k*=5 (a through d, respectively) based on size-corrected and standardized skull measurements. Clusters are represented by symbols but are not hierarchical, thus symbols do not represent the same clusters across panels. Populations are labeled by the subspecies they represent, as coded in Fig. 1. The range of *N. cinerea* is shaded grey, and the white dashed line is the approximate boundary between the two major phylogenetic clades. The solid black lines show the Columbia and Snake rivers in the northwest and the Green and Colorado rivers in the southeast



body sizes in colder climates (Bergmann 1847; Brown and Lee 1969; Smith et al. 1995; Smith and Betancourt 2006), the ANCOVA results suggest the size difference between the two clades exists merely because the Western clade has a greater northern latitudinal extent encompassing colder climates. Although insignificant due to the conservative Bonferroni corrections ($\alpha=0.0045$), the Western clade specimens also have marginally longer molar rows ($t_{df=60.8}=-2.72$, $P=0.009$), and the Eastern clade specimens have marginally wider occipital breadths ($t_{df=68.3}=2.43$, $P=0.018$). As the auditory bullae and the mastoid processes

used to measure occipital breadth are in close morphological proximity, it is not surprising that bullar size and occipital breadth are positively correlated (linear regression $P<0.001$, $df=212$, $R^2=0.05$) and show similar trends of larger size in the Eastern clade specimens.

PCA was restricted to specimens with a full complement of measured variables ($n=156$), and MANOVA and DFA were further restricted to specimens with a priori regional classification ($n=149$). The first four principal components (PC) were presumably informative with eigenvalues >1 (Table 3). However, the plot of PC2 against PC1 showed

Table 2 *T*-tests of size-corrected and standardized craniodental measurements comparing *N. cinerea* specimens from the major Eastern and Western clades. Mean *Z*-scores for each variable indicate the direction of difference between the clades. Variable means in untransformed mm (+/− standard deviation) are shown for each sex in each region. Significant *P*-values with Bonferroni correction ($\alpha=0.0045$) are bolded

Variable	<i>t</i>	<i>df</i>	<i>P</i>	Eastern mean <i>Z</i> -score	Eastern F mean	Eastern M mean	Western mean <i>Z</i> -score	Western F mean	Western M mean
Basilar length	−3.81	66.6	< 0.001	−0.488	38.75 (2.52)	39.21 (3.36)	0.113	40.54 (2.40)	41.99 (3.46)
Nasal length	−0.21	60.4	0.833	−0.058	18.33 (1.31)	18.62 (1.69)	−0.020	19.36 (1.34)	19.87 (1.53)
Rostrum width	0.71	77.9	0.483	0.059	4.54 (0.23)	4.77 (0.32)	−0.040	4.71 (0.29)	4.85 (0.33)
Rostrum depth	−0.79	53.1	0.431	−0.155	7.68 (0.44)	7.97 (0.58)	0.011	8.10 (0.44)	8.40 (0.64)
Interorbital breadth	0.48	59.8	0.635	0.067	5.72 (0.25)	5.83 (0.28)	−0.012	5.74 (0.25)	5.76 (0.27)
Palatal bridge length	1.72	68.3	0.090	0.198	8.70 (0.54)	8.93 (0.65)	−0.068	8.79 (0.62)	9.09 (0.72)
Molar row length	−2.72	60.8	0.009	−0.384	9.47 (0.37)	9.66 (0.39)	0.082	9.75 (0.43)	9.91 (0.42)
Zygomatic breadth	−1.41	57.5	0.164	−0.221	23.96 (1.45)	24.26 (1.87)	0.034	25.06 (1.40)	25.75 (1.75)
Occipital breadth	2.43	68.3	0.018	0.309	19.05 (0.79)	19.43 (1.12)	−0.076	19.48 (0.76)	20.15 (1.06)
Bullar length	6.10	73.8	< 0.001	0.705	7.72 (0.42)	7.83 (0.42)	−0.183	7.61 (0.36)	7.76 (0.49)
Interpterygoid fossa width	−3.29	72.7	0.002	−0.398	2.83 (0.26)	2.81 (0.19)	0.092	3.05 (0.24)	3.01 (0.31)

only slight separation of the major Eastern and Western clades evident in different centers of density (Fig. 5a), and plots of the other informative PCs (not shown) provided no greater qualitative separation. The inflection point in the proportion of variance explained across PCs (Table 3) was at PC2 (scree plot not shown), so we included both PC1 and PC2 in the MANOVA model assessing component scores for each specimen as a function of clade. Clade did not predict PC1 score ($F=1.34, P=0.25$), but it did significantly predict PC2 score ($F=6.89, P=0.01$). Although PC2 explained only 13.9 % of the variance in the dataset, its loadings (Table 3) are similar to patterns uncovered in the *t*-tests (Table 2). Of variables showing at least marginal significance ($P \leq 0.10$) in the *t*-tests prior to Bonferroni correction, longer auditory bullae, larger occipital breadth, and longer palatal bridge were loaded toward the positive end of

the axis where the Eastern clade specimens are concentrated; in contrast to the *t*-test results, longer molar row was also loaded toward the positive end of the axis with the Eastern clade. Wider interpterygoid breadth was loaded toward the negative end of the axis where the Western clade specimens are concentrated. Like PC2, the loadings in the single linear discriminant eigenvector (Table 3) are similar to patterns uncovered in the *t*-tests. Longer auditory bullae, larger occipital breadth, and longer palatal bridge are loaded toward the negative end of the discriminant axis with the Eastern clade (Table 3; Fig. 5b), while wider interpterygoid fossa and longer molar row were loaded toward the positive end of the discriminant axis with the Western clade (Table 3; Fig. 5b). Classification accuracy determined per specimen from jackknife analyses was 72.5 % overall and 21.4 % and 84.3 % within the Eastern and Western clades, respectively.

Table 3 Eigenvalues, percent of variance explained, and variable loadings of the first 5 principal components (PCs), and variable loadings of the linear discriminant function analysis (LD), from multivariate analyses of size-corrected and standardized craniodental measurements from *N. cinerea*. Empty cells are loadings <|0.10|

	PC1	PC2	PC3	PC4	PC5	LD
Eigenvalue	1.39	1.18	1.12	1.04	0.97	n/a
Variance explained (%)	19.5	13.9	12.6	10.9	9.4	n/a
Nasal length	0.22	−0.48	−0.10	−0.34	−0.19	
Rostrum width	0.31		0.12	0.19		
Rostrum depth	0.46	−0.46		−0.24		
Interorbital breadth	0.38		−0.16	0.56	0.52	−0.21
Palatal bridge length	0.24	0.49	−0.15	−0.53	0.27	−0.28
Molar row length	0.23	0.35	0.57	−0.29		0.47
Zygomatic breadth	0.48		−0.24			0.51
Occipital breadth	0.37	0.18	−0.13	0.24	−0.49	−0.15
Bullar length	0.12	0.27	0.21	0.18	−0.59	−0.91
Interpterygoid fossa width	0.10	−0.28	0.70	0.16	0.11	0.40

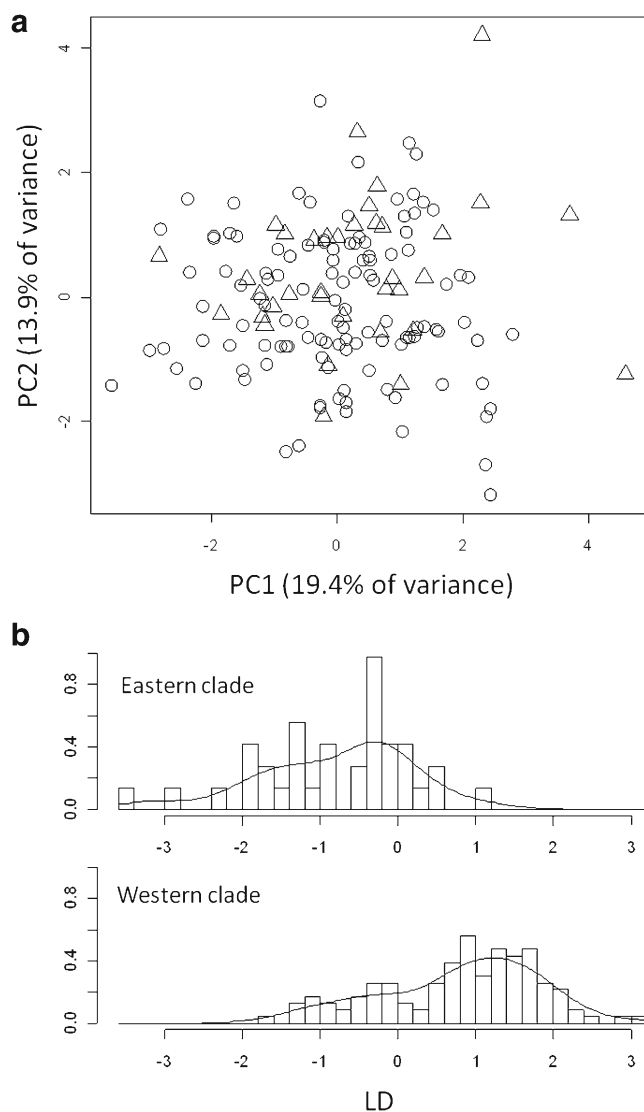


Fig. 5 Multivariate analysis plots comparing size-corrected and standardized skull measurements of specimens of the 2 major *N. cinerea* clades. **a** plot of the first two principal component (PC) eigenvectors from principal component analysis, with clades labeled by symbol: triangles, Eastern clade; circles, Western clade. **b** histograms and associated smoothed density plots of the Eastern and Western clade specimens against the single linear discriminant (LD) eigenvector from differential factor analysis

Qualitatively, we did not detect spatial trends in misclassification for either clade.

Lastly, our third question was how morphometric variation among subspecies was related to patterns between the two major clades. Tukey-Kramer contrasts of the morphometric data (Online Resource 2) helped identify finer-scale patterns underlying observed differences between the Eastern and Western clades in several features. The *t*-test showing marginally wider occipital breadth in specimens of the Eastern clade may have been influenced primarily by *N. c. orolestes*, which shows significantly wider occipital breadth

than several Western clade subspecies. Consistent with the *t*-test showing significantly longer auditory bullae in the Eastern clade, all contrasts between Eastern and Western subspecies reaching at least marginal significance ($P \leq 0.1$) showed that Eastern subspecies have longer bullae. Western clade *N. c. acraea* specimens are unusual in that they also show significantly longer bullae ($P \leq 0.05$) than many of the other Western subspecies; further, *N. c. acraea* differs significantly from all Western clade subspecies in at least one variable but does not differ from Eastern clade subspecies in any variable. As such, *N. c. acraea* is more similar morphometrically to the Eastern group subspecies than the Western group, a pattern that is also evident in the *k*-means clustering results (Fig. 4).

All contrasts in body size (i.e., basilar length) between Eastern and Western subspecies reaching at least marginal significance showed that the Western subspecies are larger than Eastern. However, most of these contrasts specifically showed that specimens of the higher-latitude subspecies (i.e., *N. c. cinerea*, *N. c. occidentalis*, and *N. c. saxamans*) were larger than lower-latitude subspecies, which is consistent with the ANCOVA results implicating high latitudes as the primary influence on body size rather than clade (described above). The significantly wider interpterygoid fossae in Western clade specimens may have been influenced by Western clade *N. c. alticola*, which shows significantly wider fossae than two of the Eastern clade subspecies. The marginally longer molar rows in specimens of the Western clade may have been influenced by Western clade *N. c. alticola* and *N. c. fusca*, which show significantly longer molar rows than several subspecies in both Eastern and Western clades. Although the *t*-test trend of longer palatal bridges in the Western clade specimens was insignificant ($t_{df=68.3}=1.72$, $P=0.090$), it may have been influenced by *N. c. fusca*, which has significantly longer palatal bridges than all other subspecies in both clades.

SPV morphology is largely consistent with historical subspecies descriptions (Table 1). Specimens of Eastern clade (*N. c. orolestes* group) subspecies show almost exclusively open SPVs, while specimens of Western clade (*N. c. occidentalis* group) subspecies show almost exclusively narrow or closed SPVs. We note that *N. c. saxamans* shows a much larger proportion of open SPVs than *N. c. occidentalis* (Osgood 1900; Goldman 1910), with which it was synonymized (Cowan and Guiguet 1956).

Discussion

We find strong concordance between the historically described *N. c. orolestes* and *N. c. occidentalis* groups and the major Eastern and Western cyt *b* clades, respectively, as is evident in patterns of SPV morphology both geographically

(Fig. 3a) and phylogenetically (Fig. 3b). SPVs vary developmentally and/or phylogenetically within *Neotoma* species (Allen 1894a; this study), among *Neotoma* species (Merriam 1894a; True 1894), within Neotomini (Merriam 1894a), and among neotomine-peromyscine rodents (Steppan 1995), but often remain useful for phylogenetic purposes (Burt and Barkalow 1942; Carleton 1980; Steppan 1995). Little is known regarding the possible function or effects of different SPV forms. In lagomorphs, a small sulcus associated with the SPV is the passageway for the nerve of the pterygoid canal (Wible 2007), while in some rodents, unossified SPVs are covered by a membrane separating the cranial cavity from the pharynx (Rickart et al. 1998). The fact that SPV form differs across taxonomic levels, particularly in neotomine-peromyscine rodents, could support our assumption that SPV form has no significant effect on fitness in this taxon and thus could evolve neutrally. Here, the agreement between SPV and phylogeny—based on the also presumed selectively neutral *cyt b* changes—illustrates two lines of evidence for divergence in *N. cinerea*, estimated by molecular data to have occurred near the Pliocene-Pleistocene transition (Hornsby and Matocq 2012).

As in the major phylogenetic clades, *N. cinerea* SPV patterns exhibit a sharp transition at the Colorado and Green rivers in the southern portion of the species distribution, as hypothesized by Goldman (1910). In this area, the Eastern clade (*N. c. orolestes* group) subspecies have open SPVs (Merriam 1894b; Goldman 1910; Hooper 1944; Kelson 1949) and the Western clade (*N. c. occidentalis* group) subspecies have closed SPVs (Goldman 1910; Hooper 1940). These descriptions are consistent with our data except for low frequencies of narrow SPVs across the Great Basin and Sierra Nevada (Fig. 3a), which Hooper (1940) may have observed in some specimens though their locations were not specified.

Further north in Montana, the narrow and presumably intermediate SPV morphology predominates. This may be indicative of admixture between the major clades at their interface. Several specimens of the Western mitochondrial clade have narrow SPVs, but no specimens of the Eastern clade have narrow or closed SPVs (Fig. 3b); thus, we tentatively hypothesize stronger mitochondrial introgression from the Western clade into populations containing open SPVs indicative of Eastern clade morphology. However, this pattern is based on very few samples and no nuclear genetic markers. Narrow SPVs also predominate in parts of British Columbia, Oregon, and northern California, and are found at lower frequencies across most of the Western clade distribution. Open SPVs are rare in the Western clade, with the exception of specimens from northern British Columbia and Yukon. This is consistent with historical descriptions of the subspecies in that region, *N. c. saxamans*, as having open SPVs (Osgood 1900; Goldman 1910); however, *N. c.*

saxamans has since been synonymized with *N. c. occidentalis* (Cowan and Guiguet 1956), which generally has narrow or closed SPVs (Table 1; Goldman 1910; Hooper 1940). Several explanations are possible for the predominance of open SPVs in the far north of the species range: (1) character reversal during northward postglacial dispersal; (2) founder effect during northward postglacial dispersal; or (3) population persistence in a northern glacial refugium, which has not yet been indicated for *N. cinerea* in molecular patterns (Hornsby and Matocq 2012) or niche models (Waltari and Guralnick 2009).

In contrast to the association of SPV morphology with major mitochondrial clades, we found weak evidence that specimens of the Eastern and Western clades show consistent craniodental morphometric differences. Our PCA and DFA did not definitively separate or classify the clades. The significant contrasts between clades may have been influenced by select subspecies displaying relatively extreme morphologies, such as the long molar rows which have been noted in *N. c. alticola* and *N. c. fusca* (Hooper 1940). The *k*-means clustering and contrasts between subspecies suggest that *N. c. acraea* is more similar morphometrically to Eastern clade subspecies at the same latitudes—but on the opposite side of the Green and Colorado rivers—than it is to Western clade subspecies. This pattern may be influenced in particular by the large bullae in *N. c. acraea*, which has previously been noted (Goldman 1910). Finley (1958), also reported morphological similarities across the Colorado River, suggesting that *N. c. acraea* and *N. c. alticola* differed from *N. c. arizonae* primarily in SPV form. Similarly, Long (1965) noted that morphological similarities between *N. c. cinnamomea* and *N. c. rupicola* may be the result of convergent responses to arid climates.

We suspect that convergent evolution has similarly occurred at lower latitudes in the Eastern and Western clades, specifically in overall body size in accordance with Bergmann's Rule (Bergmann 1847; Mayr 1956; Brown and Lee 1969; Smith et al. 1995; Smith and Betancourt 2006) and hypertrophy of the auditory bullae as an adaptive response to open or arid environments (Webster and Webster 1971; Lay 1972; Cordero and Epps 2012). Of course, there are several ways by which these groups may have become morphologically similar without the independent emergence of similar morphologies. One possible scenario is that the two clades once comprised a single, continuous geographic unit, which already showed these clines in body size and bullar size, and which was later divided through formation of the Colorado and Green rivers with mitochondrial lineages sorting stochastically into the two clades we see today. In this case, the body size and bullar size clines would be homologous. Considering that the divergence date between the two clades is estimated at 2.77 million years ago (Hornsby and Matocq 2012) and at least the upper

Colorado River is thought to have been in place for over 6 million years (Howard and Bohannon 2001), this hypothesis of *N. cinerea* division is not biogeographically plausible. Another scenario is that the Pleistocene avulsions of the lower Colorado river essentially shifted low latitude *N. cinerea* populations to the opposite side of the river (e.g., Hoffmeister and Lee 1967; Mulcahy et al. 2006; Jezkova et al. 2009) to allow gene flow. In this case, morphological similarities could be due to homologous shared alleles. This is more plausible than the first scenario, particularly as *N. cinerea* ranged farther south during the Pleistocene glacial periods than it does today (Harris 1984, 1993) and thus could have been in areas where these avulsions occurred. However, the complete separation of clades across the Colorado River and lack of intermediate SPV morphologies in this region suggest that no gene flow has occurred across this barrier. A final scenario is of independent emergence of similar phenotypes between the two clades in similar environments across the Colorado River, which is the most consistent with observed genetic and SPV patterns.

Whether we refer to this morphological similarity as the product of convergent evolution or parallel evolution is a nuanced point (Kocher et al. 1993). The *N. cinerea* clades show regional morphological convergence in the broad sense, but use of the term “convergent evolution” usually suggests that the taxa in question have different antecedents; that is, the taxa are not closely related and it seems likely that their similarities are the result of different alleles or developmental pathways. The term “parallel evolution” is often invoked when the taxa have the same antecedent, for instance a shared ancestral gene pool, through which the same alleles and pathways could be shaped by similar selective forces in parallel. Arendt and Reznick (2008) argue that this is a false dichotomy, as recent molecular data show that distantly related taxa may converge by the same pathways just as closely related taxa may converge through different ones. Whether we believe convergence and parallelism should be recognized as distinct processes or not, the modes by which divergent taxa develop convergent phenotypes will shed light on our understanding of how taxa change to meet environmental challenges. It may specifically have implications for our understanding of the evolutionary lability of this and other taxa with respect to climatic changes in both temperature and precipitation.

Conclusion

At the broadest spatial scale within *N. cinerea*, our concordant mitochondrial and SPV patterns reveal a clear east–west separation of groups across the Colorado and Green Rivers. In contrast, our morphometric analyses show a

north–south subdivision in overall variation. This discordance is somewhat surprising given the moderately high level of subdivision in mitochondrial *cyt b* variation (uncorrected p-distance 6.5 %, corrected 8.8 %). This falls in the range thought to indicate potential species-level *cyt b* divergence across small mammals (corrected 2–11 %; Bradley and Baker 2001) and is typical of that seen between sister species of Rodentia (corrected 1.3–13.0 %, mean 7.3 %; Baker and Bradley 2006). Recent studies of related *Neotoma* taxa have revealed species-level subdivisions between *N. fuscipes* and *N. macrotis* (p-distance 11 %, Matocq 2002) and *N. bryanti* and *N. lepida* (p-distance 9 %, Patton et al. 2008). The *cyt b* divergences between sister species in these complexes are accompanied by trenchant differences in qualitative morphological features and morphometric patterns, as well as substantive divergence at nuclear loci (Matocq 2002; Patton et al. 2008). *Cyt b* divergence in *N. cinerea* is close to the levels of divergence observed in these systems, yet the patterns of mitochondrial and morphometric variation are discordant. This suggests that while some characters like mtDNA and SPV, both perhaps neutral relative to selection, diverged via drift during periods of vicariance, overall craniodental variation has been shaped by environmental clines resulting in similar morphologies between distantly related populations.

Acknowledgments For assistance in the field we thank J. Daggett, J. Bender, H. Squires, J. Crawford, and R. Engel. We kindly thank C. Conroy for his extensive help in, among other things, cleaning and acquiring specimens, and to the additional staff and curators of the following museums for specimen loans: Brigham Young University Monte L. Bean Life Science Museum; Denver Museum of Nature and Science; Field Museum of Natural History; University of California, Berkeley, Museum of Vertebrate Zoology; University of Puget Sound Slater Museum; Royal Alberta Museum; Royal British Columbia Museum; Royal Ontario Museum; University of Alaska-Fairbanks Museum of the North; University of Colorado Museum of Natural History; University of Michigan Museum of Zoology; University of Utah Museum of Natural History; University of Washington Burke Museum. We thank P. Murphy for statistical assistance, and B. Coyner, A. de Queiroz, C. Feldman, M. Gritts, G. Hoelzer, S. Mensing, and the University of Nevada EECB peer review group for help and comments on early drafts. This paper was greatly improved by thoughtful input from D. Huckaby. This research was supported in part by: National Science Foundation DEB-0644371 and DEB-0952946 to M.D.M., an American Society of Mammalogists Grants-in-Aid of Research to A.D.H., and a National Science Foundation Nevada Experimental Program to Stimulate Competitive Research (EPSCoR) Graduate Fellowship to A.D.H. (through EPS-0814372).

References

- Adams CE, Woltering C, Alexander G (2003) Epigenetic regulation of trophic morphology through feeding behaviour in Arctic charr, *Salvelinus alpinus*. *Biol J Linn Soc* 78:43–49

- Allen JA (1894a) Cranial variations in *Neotoma micropus* due to growth and individual differentiation. Bull Am Mus Nat Hist 6:233–247
- Allen JA (1894b) Descriptions of ten new North American mammals, and remarks on others. Bull Am Mus Nat Hist 6:317–332
- Allen JA (1895) Descriptions of new American mammals. Bull Am Mus Nat Hist 7:327–340
- Allen JA (1903) Mammals collected in Alaska and northern British Columbia by the Andrew J. Stone expedition of 1902. Bull Am Mus Nat Hist 19:521–567
- Arendt J, Reznick D (2008) Convergence and parallelism reconsidered: what have we learned about the genetics of adaptation? Trends Ecol Evol 23:26–32
- Baird SF (1857) Reports of Explorations and Surveys to Ascertain the Most Practicable and Economical Route for a Railroad from the Mississippi River to the Pacific Ocean. A. O. P. Nicholson, Washington.
- Baker RJ (1984) A sympatric cryptic species of mammal: a new species of *Rhogeessa* (Chiroptera, Vespertilionidae). Syst Zool 33:178–183
- Baker RJ, Bradley RD (2006) Speciation in mammals and the genetic species concept. J Mammal 87:643–662
- Bergmann C (1847) Über die Verhältnisse der Wärmeökonomie der Thiere zu ihrer Grösse. Gött Stud 3:595–708
- Bickford D, Lohman DJ, Sodhi NS, Ng PKL, Meier R, Winker K, Ingram KK, Das I (2007) Cryptic species as a window on diversity and conservation. Trends Ecol Evol 22:148–155
- Bradley RD, Baker RJ (2001) A test of the genetic species concept: cytochrome-*b* sequences and mammals. J Mammal 82:960–973
- Brown JH, Lee AK (1969) Bergmann's rule and climatic adaptation in woodrats (*Neotoma*). Evolution 23:329–338
- Burt WH (1934) The mammals of southern Nevada. Trans San Diego Soc Nat Hist 7:375–428
- Burt WH, Barkalow FS (1942) A comparative study of the bacula of wood rats (Subfamily Neotominae). J Mammal 23:287–297
- Carleton MD (1980) Phylogenetic relationships in neotomine-peromyscine rodents (Muroidea) and a reappraisal of the dichotomy within New World Cricetinae. Misc Publ Mus Zool Univ Mich 157:1–146
- Carleton MD, Musser GG (2005) Order rodentia. In: Wilson DE, Reeder DM (eds) Mammal Species of the World, 3rd edn. The Johns Hopkins University Press, Baltimore, pp 745–752
- Cordero GA, Epps CW (2012) From desert to rainforest: phenotypic variation in functionally important traits of bushy-tailed woodrats (*Neotoma cinerea*) across two climatic extremes. J Mammal Evol 19:135–153
- Coues E (1877) Monographs of North American Rodentia: No. 1 – Muridae. In: Hayden FV (ed) Report of the United States Geological Survey of the Territories. Government Printing Office, Washington, pp 1–264
- Cowan IM, Guiguet CJ (1956) The Mammals of British Columbia, 1st edn. D. McDiarmid, Victoria, B.C.
- Derkarabetian S, Ledford J, Hedin M (2011) Genetic diversification without obvious genitalic morphological divergence in harvestmen (Opiliones, Laniatores, *Sclerobunus robustus*) from montane sky islands of western North America. Mol Phylogenet Evol 61:844–853
- Drummond AJ, Rambaut A, Shapiro B, Pybus OG (2005) Bayesian coalescent inference of past population dynamics from molecular sequences. Mol Biol Evol 22:1185–1192
- Edwards CW, Bradley RD (2002) Molecular systematics of the genus *Neotoma*. Mol Phylogenet Evol 25:489–500
- Escherich PC (1981) Social biology of the bushy-tailed woodrat. Univ Calif Publ Zool 110:1–132
- Finley RBJ (1958) The wood rats of Colorado. Univ Kansas Publ Mus Nat Hist 10:213–552
- Goldman EA (1910) Revision of the wood rats of the genus *Neotoma*. N Am Fauna 31:1–122
- Goldman EA (1917) New mammals from North and Middle America. Proc Biol Soc Wash 30:107–116
- Gray JE (1843) List of the Specimens of Mammalia in the Collection of the British Museum. George Woodfall and Son, London
- Hall ER (1981) The Mammals of North America. John Wiley and Sons, New York
- Harris AH (1984) *Neotoma* in the late Pleistocene of New Mexico and Chihuahua. Spec Publ Carnegie Mus Nat Hist 8:164–178
- Harris AH (1993) Quaternary vertebrates of New Mexico. New Mex Mus Nat Hist Sci Bull 2:179–197
- Hey J (2010) Isolation with migration models for more than two populations. Mol Biol Evol 27:905–920
- Hillis DM, Dixon MT, Jones AL (1991) Minimal genetic variation in a morphologically diverse species (Florida tree snail, *Liguus fasciatus*). J Hered 82:282–286
- Hoffmeister DF, Lee MR (1967) Revision of pocket mice, *Perognathus penicillatus*. J Mammal 48:361–380
- Hooper ET (1940) Geographic variation in bushy-tailed wood woodrats. Univ Calif Publ Zool 42:407–424
- Hooper ET (1944) General notes: the name *Neotoma cinerea cinnamomea* Allen applied to woodrats from southwestern Wyoming. J Mammal 5:415
- Hornsby AD, Matocq MD (2012) Differential regional response of the bushy-tailed woodrat (*Neotoma cinerea*) to late Quaternary climate change. J Biogeogr 39:289–305
- Howard KA, Bohannon RG (2001) Lower Colorado River: Upper Cenozoic deposits, incision, and evolution. In: Young RA, Spamer EE (eds) Colorado River: Origin and Evolution. Grand Canyon Association, United States of America, pp 101–105
- Jezkova T, Jaeger JR, Marshall ZL, Riddle BR (2009) Pleistocene impacts on the phylogeography of the desert pocket mouse (*Chaetodipus penicillatus*). J Mammal 90:306–320
- Kelson KR (1949) Two new wood woodrats from eastern Utah. J Wash Acad Sci 39:417–419
- Kocher TD, Conroy JA, McKaye KR, Stauffer JR (1993) Similar morphologies of cichlid fish in lakes Tanganyika and Malawi are due to convergence. Mol Phylogenet Evol 2:158–165
- Lay D (1972) The anatomy, physiology, functional significance and evolution of specialized hearing organs of gerbilline rodents. J Morphol 138:41–120
- Lemey P, Rambaut A, Drummond AJ, Suchard MA (2009) Bayesian phylogeography finds its roots. PLoS Comput Biol, 5:e1000520. doi: 10.1371/journal.pcbi.1000520
- Long CA (1965) The mammals of Wyoming. Univ Kansas Publ Mus Nat Hist 14:493–758
- Losos JB, Jackman TR, Larson A, de Queiroz K, Rodriguez-Schettino L (1998) Contingency and determinism in replicated adaptive radiations of island lizards. Science 279:2115–2118
- Matocq MD (2002) Morphological and molecular analysis of a contact zone in the *Neotoma fuscipes* species complex. J Mammal 83:866–883
- Matocq MD, Murphy PJ (2007) Fine-scale phenotypic change across a species transition zone in the genus *Neotoma*: disentangling independent evolution from phylogenetic history. Evolution 61:2544–2557
- Mayr E (1956) Geographical character gradients and climatic adaptation. Evolution 10:105–108
- Merriam CH (1893) Two new woodrats from the plateau region of Arizona (*Neotoma pinetorum* and *N. arizonae*), with remarks on the validity of the genus *Teonoma* of Gray. Proc Biol Soc Wash 8:109–112
- Merriam CH (1894a) A new subfamily of Murine rodents—the Neotominae—with description of a new genus and species and a synopsis of the known forms. Proc Acad Nat Sci Phila 46, 225–252
- Merriam CH (1894b) Abstract of a study of the American wood rats, with descriptions of fourteen new species and subspecies of the genus *Neotoma*. Proc Biol Soc Wash 9:117–128

- Mulcahy DG, Spaulding AW, Mendelson JR, Brodie ED (2006) Phylogeography of the flat-tailed horned lizard (*Phrynosoma mcallii*) and systematics of the *P. mcallii-platyrrhinus* mtDNA complex. *Mol Ecol* 15:1807–1826
- Osgood WH (1900) General account of the region. In: Merriam CH (ed) Results of a Biological Reconnaissance of the Yukon River Region. Government Printing Office, Washington, pp 7–20
- Patton JL, Huckaby DG, Álvarez-Casteñeda ST (2008) [2007] The evolutionary history and a systematic revision of woodrats of the *Neotoma lepida* group. *Univ Calif Publ Zool* 135:1–411
- R Core Development Team (2011) R: a language and environment for statistical computing. R Foundation for Statistical Computing, Vienna
- Reist JD (1985) An empirical evaluation of several univariate methods that adjust for size variation in morphometric data. *Can J Zool* 63:1429–1439
- Rickart EA, Heaney LR, Tabaranza, Jr., BR, Balet DS (1998) A review of the genera *Crunomys* and *Archboldomys* (Rodentia: Muridae: Murinae), with descriptions of two new species from the Philippines. *Fieldiana Zool* 89:1–24
- Rieseberg LH, Willis JH (2007) Plant speciation. *Science* 317:910–914
- Smith FA (1997) *Neotoma cinerea*. *Mammalian Species* 564:1–8
- Smith FA, Betancourt JL (2006) Predicting woodrat (*Neotoma*) responses to anthropogenic warming from studies of the palaeomidden record. *J Biogeogr* 33:2061–2076
- Smith FA, Betancourt JL, Brown JH (1995) Evolution of body size in the woodrat over the past 25,000 years of climate change. *Science* 270:2012–2014
- Smith KL, Harmon LJ, Shoo LP, Melville J (2011) Evidence of constrained phenotypic evolution in a cryptic species complex of agamid lizards. *Evolution* 65:976–992
- Steppan SJ (1995) Revision of the tribe Phyllotini (Rodentia: Sigmodontinae), with a phylogenetic hypothesis for the Sigmodontinae. *Fieldiana Zool* 80:1–112
- Thorpe RS (1975) Quantitative handling of characters useful in snake systematics with particular reference to intraspecific variation in ringed snake *Natrix natrix* (L). *Biol J Linn Soc* 7:27–43
- Thorpe RS (1976) Biometric analysis of geographic variation and racial affinities. *Biol Rev* 51:407–452
- True FW (1894) Diagnoses of some undescribed wood woodrats (genus *Neotoma*) in the National Museum. *Proc Natl Mus* 17:1–3
- Waltari E, Guralnick RP (2009) Ecological niche modelling of montane mammals in the Great Basin, North America: examining past and present connectivity of species across basins and ranges. *J Biogeogr* 36:148–161
- Webster DB, Webster M (1971) Adaptive value of hearing and vision in kangaroo rat predator avoidance. *Brain Behav Evol* 4:310–322
- Wible JR (2007) On the cranial osteology of the Lagomorpha. *Bull Carnegie Mus Nat Hist* 93:213–234